Simultaneous Production Of MnO And Syngas From MnCO$_3$-Waste Polymer Composite Pellets

James Ransford Dankwah

Abstract: This work investigates the simultaneous production of MnO and syngas (CO + H$_2$) from mixtures of MnCO$_3$ with various waste plastics in a laboratory scale horizontal tube furnace. Cylindrical compacts of reagent grade MnCO$_3$ were heated rapidly with and without high density polyethylene (HDPE at C/O ratio = 1.0, 1.5, and 2.0) and linear low density polyethylene (LLDPE at C/O ratio 1.0) for 600 s at 1150 °C under high purity argon gas and the off gas was continuously analysed for CH$_4$, CO and CO$_2$ using an online infrared gas analyser (IR). Peaks of H$_2$ gas were detected using a gas chromatographic analyser (GC). The results indicate that blending the carbonate with the polymers before heating has a significant attenuating effect on CO$_2$ emissions. It is further reported that the observed attenuation of CO$_2$ emissions is accompanied by a simultaneous production of syngas that can be recovered as a beneficial by-product.

Index Terms: Calcination; MnCO$_3$, HDPE, LLDPE, CO$_2$ emissions, Syngas

————————————————◆————————————————

1 INTRODUCTION

Thermal decomposition (calcination) of a metal carbonate results in the production of the metal oxide and the generation of large volumes of CO$_2$ into the environment. Accordingly, industrial processes like clinker formation during the manufacture of cement and the use of carbonate ores in ferroalloy production are accompanied by direct emission of CO$_2$ to the environment and contribute immensely to the anthropogenic CO$_2$ in the atmosphere. Manganese oxide ores have traditionally been the principal source of supply for alloy smelting [1]. An expansion in the steel industry has resulted in an increase in manganese ore mining activity and the acceptance of ores containing less than 50% Mn [1] , typically among which is rhodochrosite (MnCO$_3$). It has been said that carbonate ore needs 25 percent less carbon per unit of manganese when compared with the standard mixed oxide, Mn$_3$O$_4$ [1]. The lowering of the fixed carbon per unit of manganese processed increases furnace charge resistivity and therefore enhances furnace productivity [1]. Although the calcination of metal carbonates has been fairly researched into [2-17], little or no data exist in the literature, on the effect of waste plastics blending on CO$_2$ emissions. Accordingly, aside of investigating the potential feasibility of producing MnO and syngas from MnCO$_3$-waster polymer compacts, the effect of waste polymer blending on the calcination behaviour of MnCO$_3$ is another object of this investigation.

2 EXPERIMENTAL

2.1 Raw Materials

Pulverised reagent grade manganese (II) carbonate (MnCO$_3$, assaying 44% Mn) obtained from SIGMA ALDRICH was used as the carbonate. HDPE and LLDPE were employed in this study as waste polymeric materials. Their respective chemical compositions (wt. %) are given in Table 1.

———————————————————

- *Dr. James R. Dankwah (formerly of School of Materials Science and Engineering, UNSW, Sydney, Australia) is currently a lecturer in Ferrous Metallurgy at University of Mines and Technology, Tarkwa, Ghana, PH-+233 205 802 944.*
  E-mail: jrdankwah@gmail.com

TABLE 1: CHEMICAL ANALYSIS OF CARBONACEOUS MATERIALS USED IN THIS STUDY

Component	VM	Ash	Total C	H	S
HDPE (wt %)	99.4	0.6	85.5	14.2	0.3
LLDPE (wt %)	99.7	0.3	85.5	14.3	0.2

Granules of HDPE and LLDPE were crushed to smaller sizes by using a cutting mill "Pulverisette 15" (Fritsch GmbH, Idar-Oberstein, Germany). By means of a sieve insert with 0.5 mm trapezoidal perforations in the cutting mill a particle size 450-470 µm was obtained. Fixed masses of MnCO$_3$ (~ 2.00 g) were subsequently mixed with the carbonaceous blends (at C/O molar ratio of 1.0, 1.5 and 2.0) and compacted in a die to produce cylindrical pellets (~1.2 mm thick and 15 mm diameter) (Fig. 1), by applying a load of 7.5 tonnes for 2 minutes in a hydraulic press.
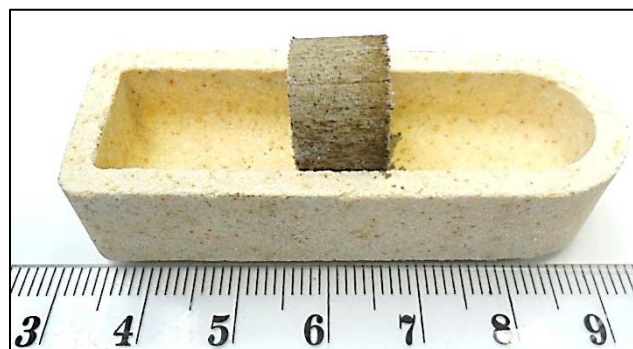

Fig. 1: MnCO$_3$-HDPE compact in a LECO® crucible before calcination

2.2 Experimental Procedure

The sample assembly was inserted in the cold zone of the furnace (Fig 2), which was purged continuously with argon (of 99.995% purity and flow rate 1.0 L/min) to ensure inert conditions. After the furnace had attained the desired hot zone temperature (1150 °C), the sample was pushed in the reaction hot zone and gases (CH$_4$, CO and CO$_2$) were monitored for 900 s by an infrared gas analyser attached to the system; the results were recorded in a data-logging computer. This time was selected since initial trials showed no significant changes in gas composition or degree of calcination beyond 900 s.

331

Peaks of H_2 were monitored and detected using a gas chromatographic (GC) analyser equipped with a thermal conductivity detector (TCD). Calcined compacts were quenched by rapidly withdrawing the tray from the hot reaction zone intothe cold zone of the furnace and were allowed to cool for 300 s under argon atmosphere to prevent oxidation of MnO to higher oxides of manganese. Calcined samples were pulverised andsubjected to SEM and XRDanalysis to confirm the presence of MnO.
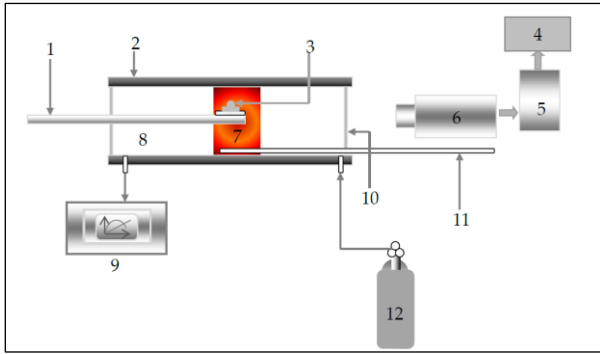

Fig. 2: Schematic of the horizontal tube furnace and IR gas analyser system. (1 Sample Rod; 2 Alumina tube; 3 Reaction mixture; 4 PC; 5 DVD; 6 CCD Camera; 7 Hot Zone; 8 Cold Zone; 9 Gas analyser; 10 Quartz window; 11 Thermocouple; 12 Argon gas)

3 Results and Discussions

3.1 Nature of the Calcined Compacts
Fig 3 shows the appearance of $MnCO_3$-HDPE compact after calcination. A complete change in appearance and size is apparent from Fig 3.
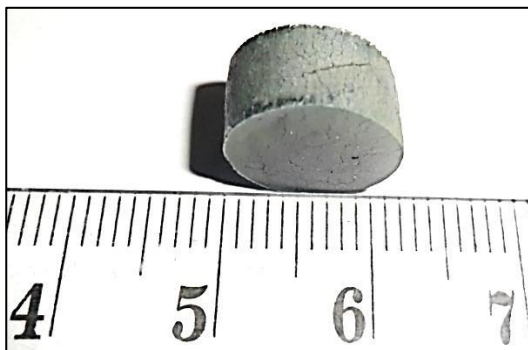

Fig. 3: $MnCO_3$-HDPE compact after calcination

Fig 4 shows the SEM image of raw $MnCO_3$ before calcination. As can be seen from Fig 4 the particles have no specific geometrical shapes. The calcined compacts are shown in Fig 5 at different magnifications for the raw carbonate, $MnCO_3$-HDPE and $MnCO_3$-LLDPE, respectively. The morphology of the calcined compacts shown in Fig 5 indicates that particles of the compacts were sintered into larger lumps in the course of calcination at 1150 ℃.
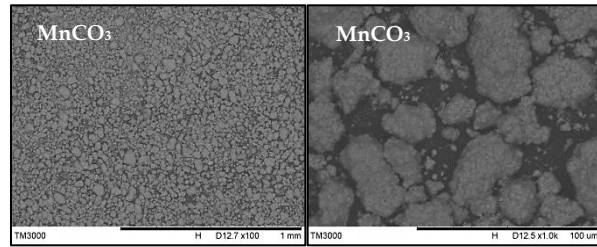

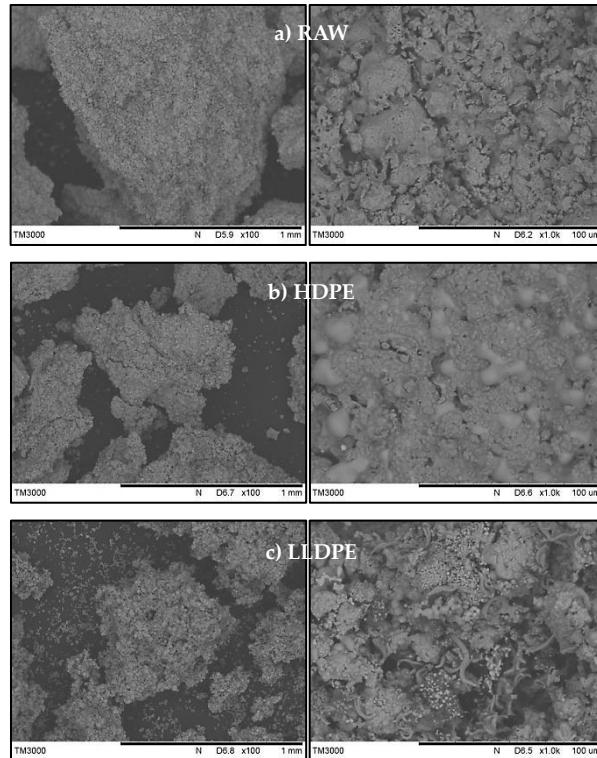**Fig. 4:** SEM of $MnCO_3$ before calcination

Fig. 5: SEM of calcined compacts: a) raw $MnCO_3$, b) $MnCO_3$-HDPE c) $MnCO_3$-LLDPE

The XRD patterns of the raw carbonate ($MnCO_3$) are shown in Fig 6 and those of the calcined compacts (MnO) are shown in Figs (7, 8 and 9) for raw $MnCO_3$, $MnCO_3$-HDPE and $MnCO_3$-LLDPE, respectively. Complete disappearance of peaks of $MnCO_3$ and appearance of distinct peaks that correspond to MnO are observed in Figs (7, 8 and 9), an indication of active calcination. The appearance of some peaks corresponding to Mn metal is apparent in Fig 8 and especially Fig 9.
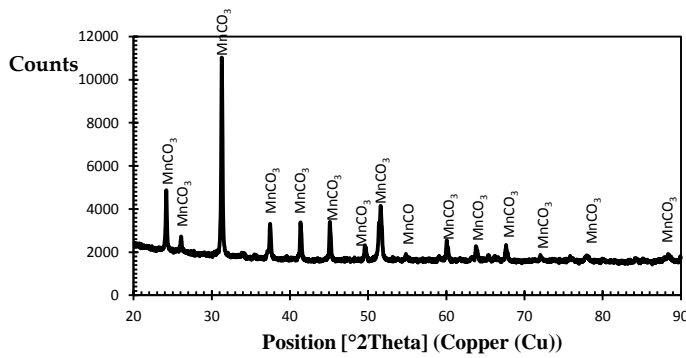
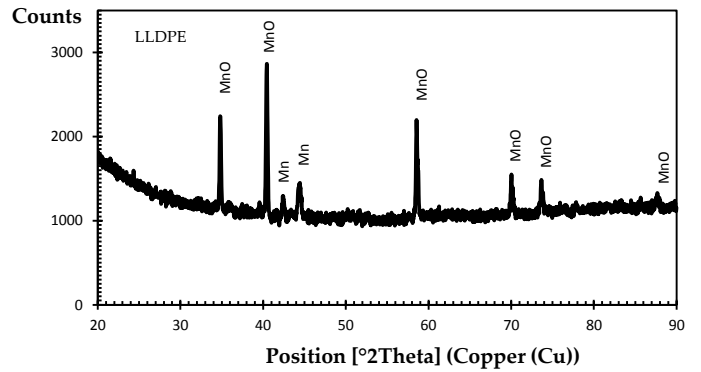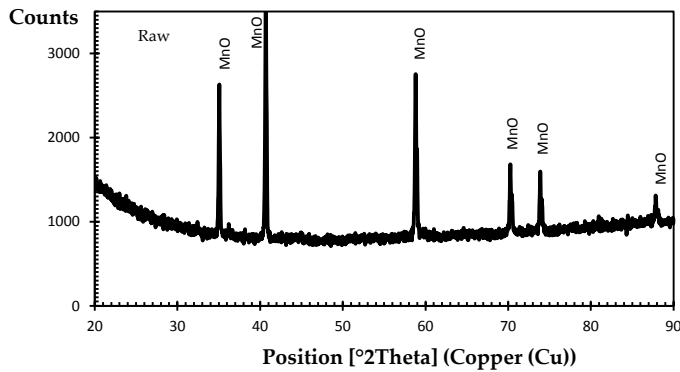**Fig. 6:** XRD of $MnCO_3$ before calcination

Fig. 7: XRD of raw $MnCO_3$ after calcination

These peaks suggest that some reduction of MnO (most likely by CH_4) to Mn did occur in the polymer-containing compacts, although the extent of such reduction reaction was minimal since temperatures higher than the experimental temperature of 1150 °C are required.

Fig. 8: XRD of $MnCO_3$-HDPE after calcination

Fig. 9: XRD of $MnCO_3$-LLDPE after calcination

3.2 IR Gas Analyses

The contents of CO, CO_2 and CH_4 in the off-gas were measured continuously by an infrared (IR) gas analyser and their concentrations were expressed in vol. %. The results are shown in Fig 10 for the raw carbonate. Gas evolution began almost immediately after inserting the raw $MnCO_3$ compact into the hot zone of the furnace, attaining maximum values of 17.99 vol. % CO_2 and 3.99 vol. % CO after 110 and 210 s, respectively. The gas generation behaviour of the carbonate-polymer compacts is illustrated in Figs (11-14) for $MnCO_3$-HDPE (C/O = 1.0), $MnCO_3$-HDPE (C/O = 1.5), $MnCO_3$-HDPE (C/O = 2.0) and $MnCO_3$-LLDPE (C/O = 1.0), respectively. At C/O = 1.0, gas generation by $MnCO_3$-HDPE compact commenced after about 90 s, attaining maximum values of 9.92 vol. % CO_2 and 15.53 vol. % CO after 120 and 240 s, respectively (Fig 11). Blending of the carbonate with the polymer resulted in a significant decrease in the CO_2 content and an increase in the CO content of the off gas.
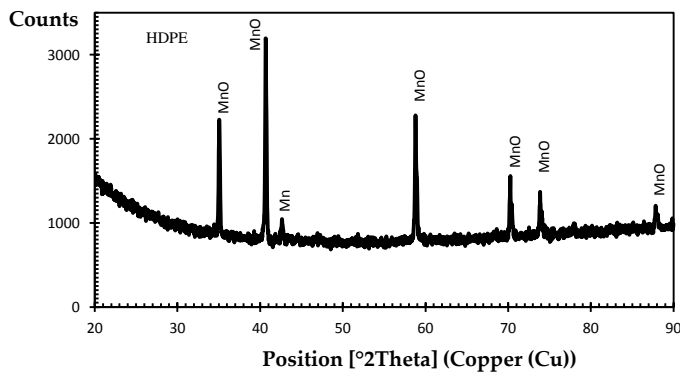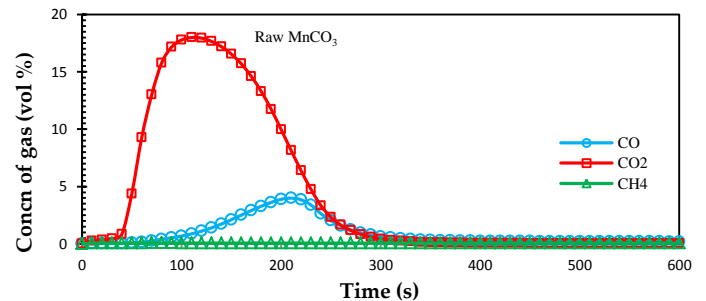

Fig. 10: Gas generation behaviour during the calcination of $MnCO_3$ compact
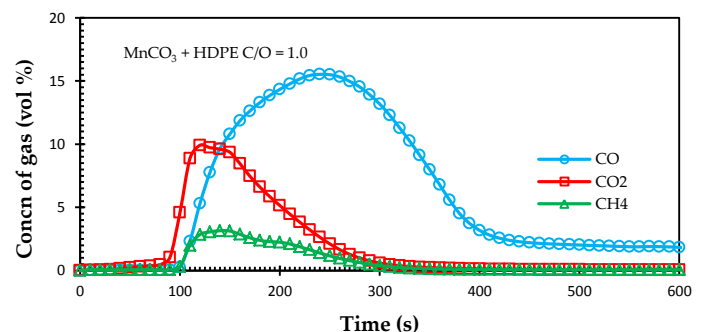

Fig. 11: Gas generation behaviour during the calcination of $MnCO_3$-HDPE compact (C/O = 1.0)

Increasing the amount of polymer results in a decrease in the maximum levels attained by CO from 15.53 vol. % (C/O = 1.0) to 14.18 vol. % and 13.17 vol % for C/O = 1.5 and C/O = 2.0, respectively, as shown in Figs (12 and 13). The maximum CO_2 levels also declined from 9.92 vol. % (C/O = 1.0) to 7.99 vol. % and 7.73 vol. % for C/O = 1.5 and C/O = 2.0, respectively. However, the maximum CH_4 content increased from 3.15 vol. % to 3.91 vol. % and 6.42 vol. % for C/O = 1.5 and C/O = 2.0, respectively.
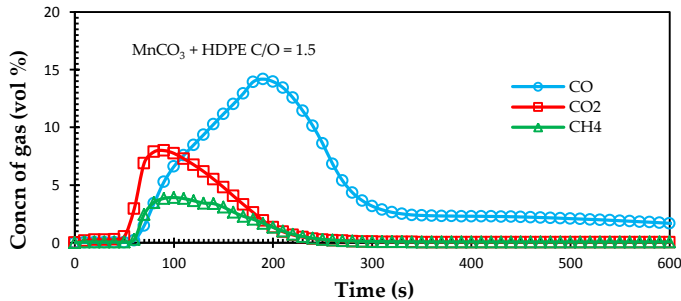

Fig. 12: Gas generation behaviour during the calcination of $MnCO_3$-HDPE compact (C/O = 1.5)
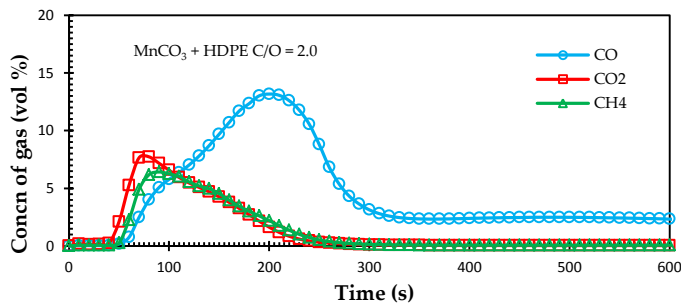

Fig. 13: Gas generation behaviour during the calcination of $MnCO_3$-HDPE compact (C/O = 2.0)

Replacing HDPE with LLDPE at the same C/O ratio did not lead to any significant change in the maximum levels of CO or CO_2. Maximum CO value dropped from 15.53 vol. % to 14.90 vol. % for LLDPE, but occurred at the same time (after 240 s). There was no difference in the maximum value of CO_2 and the time (120 s) it was evolved; 9.92 vol. % and 9.93 vol. % for HDPE and LLDPE, respectively. The striking similarities in the maximum values of CO and CO_2 by HDPE and LLDPE should not come as a surprise, judging from the chemical composition values from Table 1. However, the maximum level of CH_4 evolved showed an increase from 3.15 vol. % to 10.56 vol. %. At this stage, the difference in maximum values of CH_4 is not too clear, although they occur around the same time (after 140 s and 130 s for HDPE and LLDPE, respectively). Further research is underway to explain the discrepancy in maximum CH_4 values.
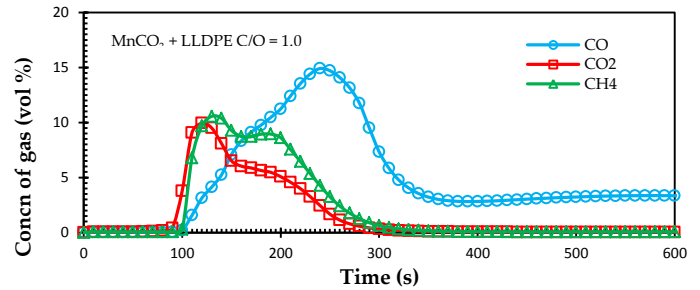

Fig. 14: Gas generation behaviour during the calcination of $MnCO_3$-LLDPE compact (C/O = 1.0)

The accumulated amount of CO evolved is shown in Fig. 15 for each compact. The highest and lowest amounts of accumulated CO evolution were observed for HDPE-containing compact (C/O = 1.0) and the raw compact, respectively. An observation of Fig. 16 shows almost the reverse situation for accumulated CO_2 emissions, with the highest amount observed for the raw compact and the lowest for the compact containing HDPE (C/O = 2.0).It was observed for iron oxide-polymer compacts that the amount of hydrogen (and therefore syngas) generated was proportional to the amount of CO evolved [18]. It means that blending the carbonate with a polymer results in a decrease in the amount of CO_2 evolved and an increase in syngas generation. Fig 17 shows the peak of H_2 gas as detected by a gas chromatographic analyser equipped with a thermal conductivity detector (TCD). The TCD detector responds to the difference between the thermal conductivity of the carrier gas and the analyte peak; the greater the difference in thermal conductivity the better the sensitivity. Argon (κ =39) was used as the carrier gas as the target analyte peak was hydrogen (κ = 419). The other gases, CO (κ =53), CO_2 (κ =34) and CH_4 (κ =73) were measured quantitatively using an IR-gas analyser. Peak determination of these gases on the chromatogram was not satisfactory since their thermal conductivities were close to argon that was used as the carrier gas.
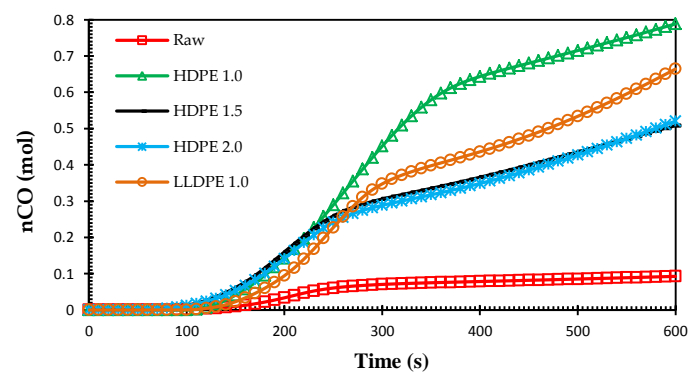

Fig. 15: Accumulated amount of CO evolved during calcination of various compacts of $MnCO_3$
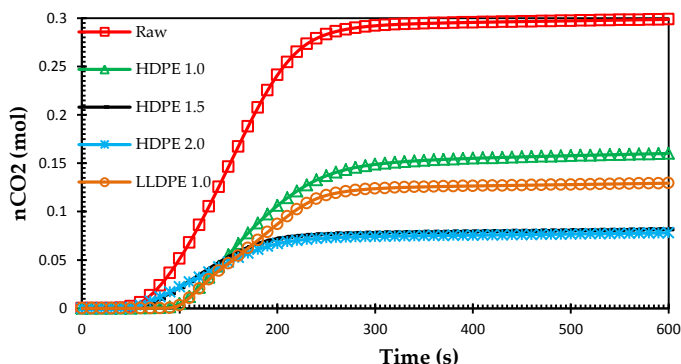
Fig. 16: Accumulated amount of CO_2 evolved during calcination of various compacts of $MnCO_3$
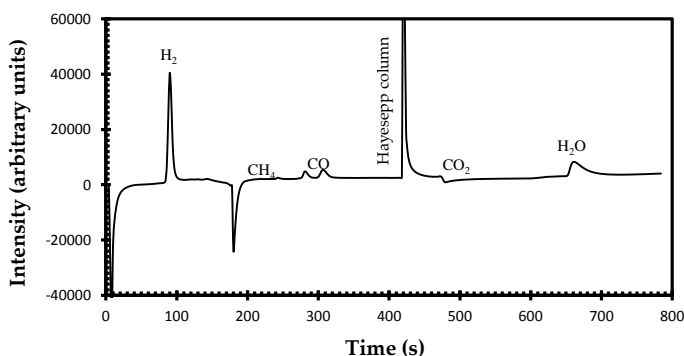

Fig. 17: Gas chromatogram obtained after calcination of $MnCO_3$-HDPE compact (C/O = 2.0) for 1 minute at 1150 °C

Combining Figs 15, 16 and 17, it can be concluded that blending the carbonate with the polymer resulted in a decrease in CO_2 emissions and an increase in syngas (CO + H_2) production.

4 CONCLUSIONS

The simultaneous production of MnO and syngas from $MnCO_3$-waste polymer blends has been investigated in a laboratory scale horizontal tube furnace at 1150 °C. It was observed that:

1) Blending the carbonate with the polymers before heating has a significant attenuating effect on CO_2 emissions.
2) Attenuation of CO_2 emissions is accompanied by a simultaneous production of syngas that can be recovered as a beneficial by-product.

ACKNOWLEDGMENT

REFERENCES

[1]   M. Compton and J. Chandler: "Elevated limestone mineral addition impacts on laboratory and field concrete performance",Concrete in Australia, vol. 38, no. 1, p. 27-33, 2012,

[2]   P. O'Shaughnessy, J.K. Kim and B.W. Lee:"The smelting of manganese carbonate ore", INFACON,vol. 10, p. 223-230, 2004

[3]   J.M. Criado, M. Gonzalez, J. Malek, and A. Ortega: "The effect of CO_2 partial pressure on the thermal decomposition kinetics of calcium carbonate", Thermochimica Acta, vol. 254, p. 121-127, 1995

[4]   J.M. Criado, M. Gonzalez and M. Macias: "Influence of CO_2 partial pressure on the kinetics of thermal decomposition of $CdCO_3$", Thermochimica Acta, vol. 113, p. 31-38, 1987

[5]   J.M. Criado, F. Gonzalez, and M. Gonzalez: "Influence of the CO_2 pressure on the kinetics of thermal decomposition of manganese carbonate", Journal of Thermal Analysis, vol. 24, p. 59-65, 1982

[6]   J. Yamaguchi, Y. Sawada, O. Sakurai, K. Uematsu, N. Mizutani and M. Kato: "Thermal decomposition of cerussite ($PbCO_3$) in carbon dioxide atmosphere (0-50 ATM)", Thermochimica Acta, vol. 35, p. 307-313, 1980.

[7]   S. Yamada, E. Tsukumo and N. Koga: "Influence of evolved gases on the thermal decomposition of zinc carbonate hydroxide evaluated by controlled rate evolved gas analysis coupled with TG", Journal of Thermal Analysis and Calorimetry, vol. 95, no. 2, p. 489-493, 2009

[8]   Z. Li, X. Shen, X. Feng, P. Wang and Z. Wu: "Non-isothermal kinetics studies on the thermal decomposition of zinc hydroxide carbonate", Thermochimica Acta, vol. 438, p. 102-106, 2005

[9]   M. Samtani, D. Dollimore, and K.S. Alexander: "Comparison of dolomite decomposition kinetics with related carbonates and the effect of procedural variables on its kinetic parameters", Thermochimic. Acta., vol. 392-393, p. 135-145, 2002

[10]   R.H. Borgwardt: "Calcination kinetics and surface area of dispersed limestone particles", J.AIChE, vol. 31, p. 103-111, 1985

[11]   P. Sun, J.R. Grace, C.J. Lim, and E.J. Anthony: "Determination of intrinsic rate constant of the CaO- CO_2 reaction", Chem. Eng. Science, vol. 63, p. 47-56, 2008

[12]   H.T. Kim, and H.B. Kwon: "Kinetic study of limestone calcination and sulfation reaction under AFBC environment", Environ. Eng. Res. , vol. 3, p. 105-113, 1998

[13]   M. Telfer, Z. Zhong, Y. Xu, D. Li, M. Zhang, and D.K. Zhang: "An experimental study of calcination of South Australian Caroline limestone", Dev. Chem. Eng. Mineral Process., vol. 8, p. 245-267, 2000

[14]   B.B. Sakadjian, M.V. Iyer, H. Gupta, and L. Fan: "Kinetics and structural characterization of calcium-based sorbents calcined under sub-atmospheric conditions for the high-temperature CO_2 capture process", Ind. Eng. Chem. Res., vol. 46, p. 35-42, 2007

[15]   Y. Wang, S. Lin, and Y. Suzuki: "Study of limestone calcination with CO_2 capture: Decomposition behavior in a CO_2 atmosphere", Energy Fuels, vol. 21, p. 3317-3321, 2007

[16]   Z. Chen, H.S. Song, M. Portillo, C.J. Lim, J.R. Grace, and E.J. Anthony: "Long-term calcination/carbonation cycling and thermal pre-treatment for CO_2 capture by limestone and dolomite", Energy Fuels, vol. 23, p. 1437-1444, 2009

[17]   P. Sun, C.J. Lim, and J.R. Grace: "Cyclic CO_2 capture by limestone-derived sorbent during prolonged calcination/carbonation cycling", J. AIChE, vol. 54, p. 1668-1677, 2008

[18]   J.R. Dankwah, "Utilisation of end-of-life plastics/rubber tyres and their blends with metallurgical coke in EAF steelmaking: reduction of iron oxide", PhD. Thesis, School of Materials Science and Engineering, University of New South Wales, Sydney, Australia, (2012).